University of Stavanger
Faculty of ...
Department of ...

Analyzing Magnetic Resonance Spectroscopy Data

Bachelor's Thesis in Computer Science

by

Johan Levent Gencher

Internal Supervisor

Morteza Esmaeili

June 15, 2023

Abstract

Magnetic resonance (MR) spectroscopy (MRS) modalities provide non-invasive and non-ionization *in vivo* imaging tools for preclinical and clinical examinations. Brain examinations' standard clinical MR protocols comprise several anatomical imaging techniques. This work describes the principal physics behind clinical MRS, spectral analysis paradigm, and MRS applications in clinical routines. The excellent contrast from the brain's anatomy partly relies on water's hydrogen nuclei relaxation time differences in tissues. Peak fitting and a linear combination of simulated metabolites are standard algorithms to estimate metabolite intensities from MR spectra. This thesis aims to implement two popular algorithms on *in vivo* clinical MR spectra and compare the quantification estimations of two methods.

Abbreviations: MR, magnetic resonance; MRS, magnetic resonance spectroscopy; NMR, nuclear magnetic resonance; FWHM, full width at half maximum; T1, spin lattice; T2, spin-spin; PPM, parts per million; T, tesla; PRESS, point-resolved spectroscopy; FID, free induction decay; FT, Fourier transformation; RF, radiofrequency field; AMARES, Advanced Method for Accurate, Robust, and Efficient Spectra; MRSI, magnetic resonance spectroscopy imaging; Cr, creatine; PCr, Phosphocreatine; GPC, Glycerylphosphocholine; NAAG, N-Acetylaspartylglutamate; SNR, signal to noise ratio; SD, standard deviation.

Keywords: magnetic resonance spectroscopy, fitting, quantification, metabolites, chemical shifts, brain chemistry.

Acknowledgements

I would like to dedicate this section of my thesis to express my appreciation to everyone who contributed to my work on this thesis. I'm immensely thankful for the open source data set made available by Jessica Archibald, her profound expertise and the generosity in sharing this data can not be underestimated. The quality of this thesis is a direct cause of the impeccable data that was provided.

I am also especially grateful for my supervisor, Mr. Morteza Esmaeili, his invaluable understanding of complex concepts and dedication to this field is nothing short of inspiring. This coupled with his guidance, patience and willingness to teach has made him a key factor to my academic journey and learning, and for that I am incredibly thankful.

Lastly, I recognize that this thesis would not have been possible without the love and support of my family and friends, who have been my constant source of motivation throughout my work. My sincere thanks go to all of you.

Contents

Chapter 1

Introduction

1.1 Introduction

This thesis aims to examine the reproducibility of previously acquired MRS data on either 3 Tesla (T) or 1.5T Point RESolved Spectroscopy (PRESS) pulse sequence and the reproducibility of the fitting outcomes. This will be done using magnetic resonance spectroscopy (MRS) specialized software to produce a table including quantified concentrations of selected metabolites. Furthermore, there will also be a brief section on the clinical applications and history of MRS. [14]

1.2 History

MSR slowly started in the 1940s and was a result of the research regarding atomic nuclei behaviour around magnetic fields. It was in 1946 that Felix Bloch and Edward Purcell independently discovered the phenomenon of NMR when atomic nuclei were placed in a magnetic field while being exposed to a specific frequency of electromagnetic radiation.

This led the early work of NMR to explore the chemical and physical properties of molecules and materials. In 1952 one of the biggest breakthroughs in NMR was made by Erwin Hahn and his technique called spin echo spectroscopy. This technique greatly improved the accuracy of NMR measurements and paved the way for more sophisticated applications.

In the 1970s and 1980s, several advances in computer technology, new magnetic materials and hardware led to rapid progress in NMR and other related techniques such as MRI and MRS. This time in history is especially important because the focus and application of these techniques started to shift towards chemical composition of biological tissues and how it could be possible to obtain information about diseases and metabolic processes. [9]

1.3 NMR versus MRS

Nuclear Magnetic Resonance (NMR) is a versatile analytical technique used in chemistry to identify molecules and determine their structure. This is done by making a spectrum of radio frequencies of each atom's nuclei resonate to the strong magnetic field that affects them. In clinical applications, the technique is referred to as MRS, with the main difference being that MRS is concerned with both identifying the molecule or metabolite and measuring its concentration. [7]

While NMR and MRS share the same underlying principle, the use of the term "nuclear" in NMR can be misleading, as it is not associated with nuclear ionizing radiation. This has led to the adoption of the term MRS to avoid confusion. The sensitivity of MRS to detect and measure metabolites makes it a valuable tool for observing subtle changes in tissue metabolites, which can be indicative of disease onset or progression. This is especially important in clinical research and practice where accurate quantification of metabolites can help in the diagnosis and monitoring of various diseases, including neurodegenerative disorders, cancers, and cardiovascular diseases. [8]

Overall, the use of MRS in clinical research and practice offers promising potential for the development of biomarkers and new insights into disease mechanisms which makes it a valuable tool for clinical research and practice, particularly in the fields of neurology, oncology, and cardiology.

1.4 MRS reproducibility and fitting

MRI and MRS technology have been available for over 30 years and show great possibilities, but they have yet to be widely adopted. The main causes are generally found to be the low spatial resolution of MRS compared to other imaging

modalities, long acquisition times required for obtaining high-quality MRS data, quality of data, inadequate analysis techniques and a general lack of awareness and appreciation from the clinical community. [17]

Simply put the key challenge is the reproducibility and consistency of MRS measurements and data. In practice problems often arise because of different hardware, software, and analysis methods, which then undermines the reliability of MRS as a resource in a clinical setting. Therefore, efforts have been made to develop standardized protocols and quality control measures to improve the reproducibility and consistency of MRS data and analysis.

The aim of these efforts is to promote wider adoption of MRS technology in clinical research and practice by providing reliable and consistent data that can be used to improve diagnostic accuracy, treatment planning, and monitoring of disease progression. As such, the development and implementation of standardized protocols and quality control measures are essential for unlocking the full potential of MRS technology in clinical practice.

This thesis aims to evaluate the different aspects of MRS data fitting, including hardware and software variations, acquisition methods, and analysis techniques, with the goal of enhancing reproducibility and consistency. By identifying areas of improvement and proposing solutions, this research aims to contribute to the wider adoption and utilization of MRS technology in clinical research and practice [1].

1.5 Outline

This thesis is divided into 5 chapters. Chapter 1 is the introduction which covers the history, the current state of MRS research, core concepts, limitations and the overall structure of this thesis. Chapter 2 builds upon the background, introduces the theory of the thesis, gives a general understanding of the different software, the biochemistry and fundamental physics of MRS. Chapter 3 Gives an in dept explanation of how the different softwares were used in this work. Chapter 4 is were the results are presented and a suggestion of these results are made. And finally, Chapter 5 looks at the results as a whole, discussing accuracy and success of the reproducibility, possible errors or improvements and the possible future of MRS research.

Chapter 1 - Introduction

Chapter 2 - Background

Chapter 3 - Materials and Methods

Chapter 4 - Results

Chapter 5 - Conclusion

Chapter 2

Background

2.1 Fitting method and theory

In the process of quantifying MRS data it is important to handle the given data properly. Meaning that a proper framework of fitting methods and analyzing is implemented. This section is therefor dedicated to exploring the most common fitting methods and their role in enhancing data interpolation and quality.

For spectral fitting there are mainly two mathematical methods that are used, the *Lorentzian* and *Gaussian* method [20]. In equation (2.1) and (2.2) F represents the Full width at half maximum (FWHM), E represents mean of the curve and h represents the height or amplitude:

$$G(x; F, E, h) = h \cdot \exp\left[-4 \ln 2 \frac{(x-E)^2}{F^2}\right] \tag{2.1}$$

$$L(x; F, E, h) = \frac{h}{1 + 4 \cdot \frac{(x-E)^2}{F^2}} \tag{2.2}$$

The Gaussian lineshape distinguishes itself with its bell-shaped curve that is symmetric and smoothly decays to zero. In the context of MRS this method is best applied to data that is well-resolved with low levels of signal loss, distortion, or asymmetry. Meaning that the width determined by the standard deviation (SD) is particularly accurate at displaying concentration values of metabolites if the signal to noise ratio (SNR) is high with a well-defined signal. Because of this there may

be some scenarios where Gaussian distribution is not ideal for the data, and it might be necessary to add asymmetry for a better fit.

While both Gaussian and Lorentzian lineshapes have a symmetrical curve, Lorentzian distinguishes itself with its more peaked curve and broader tail when comparing it to Gaussian. In principle this makes Lorentzian a better candidate for data that is distorted, asymmetric or with overlap between different peaks of metabolites. FWHM is the reason for these characteristics when using Lorentzian distribution. FWHM is the ratio between width of the peak and the maximum intensity, meaning that data with overlapping peaks due to asymmetric reading or a lower SNR can still be distinguished from one another [20].

For this reason while using both jMRUI and LCModel the SD is shown for each metabolite and for the residue. This enabels the user to choose an appropriate approach to quantifying the data and the certainty of the result. That being said LCModel does not directly use Gaussian or Lorentzian distrubution like jMRUI does, but rather a predefined basis set.

2.2 LCModel

LCModel (Linear Combination of Model spectra) is a commonly used software tool for analyzing MRS data and accurately quantifying metabolites concentrations. LCModel can analyze MRS data from nuclear magnetic resonance (NMR) or *in vivo* clinical or preclinical MRI systems.

LCModel employs a mathematical model representing the observed spectrum as a linear combination of basis spectra, which are representative of the individual metabolites. Combining different non-linear fitting algorithms, the model can estimate the contribution of each metabolite to the given MR spectrum. It enables the identification of overlapping peaks and estimation of metabolite concentrations. The platform incorporates several advanced tools to improve the analysis accuracy, such as eddy current correction, water suppression algorithms, spectral artifacts correction, and macromolecule estimations.

LCModel is used to quantitatively analyze spectra acquired from the brain, muscles, liver, prostate, and other tissues. It enables quantitative estimates of the concentrations of various metabolites in the tissue. For example, in the brain investigation, metabolites of interest include compounds such as N-acetyl-aspartate (NAA), choline-containing compounds (total Cho), creatine and phosphocreatine (tCr), glutamine, glutamate, γ-Aminobutyric acid (GABA), 2-hydroxyglutarate, lactate, and Myo-inositol. [18]

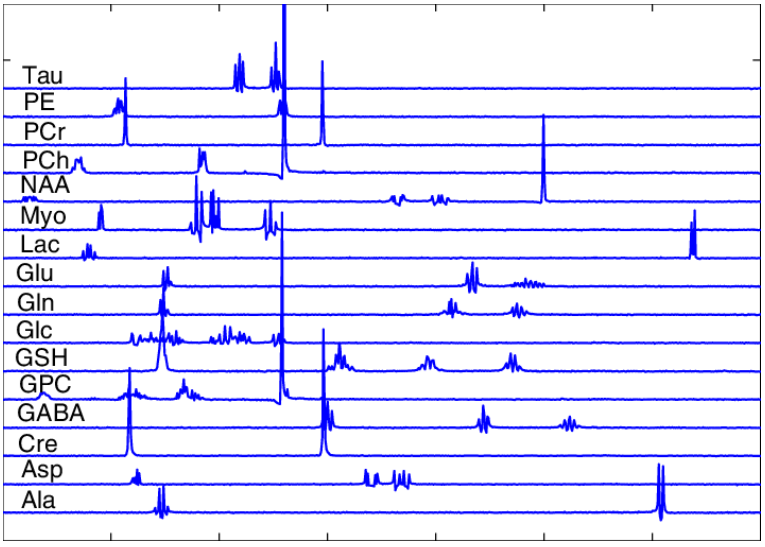

FIGURE 2.1: Basis set displaying spectra for different metabolites separately (Obtained from ResearchGate [12]).

To illustrate, an example basis set with simulated spectra for several common metabolites, including NAA, choline, creatine, and lactate is shown in **Figure 1**. These simulated spectra represent the unique spectral profiles of each metabolite, including their chemical shifts, linewidths, and amplitudes.

The basis set used by LCModel depends on the specific MRS acquisition parameters, such as the magnetic field strength, time, and vendor. LCModel includes several built-in basis sets for common metabolites, but users can also create custom basis sets for specific experimental conditions such as different organs, species or if the metabolite in question does not exist in the basis set.

2.3 jMRUI platform

jMRUI (Java-based Magnetic Resonance User Interface) is a easily accessible software for MRS processing. It provides a user-friendly interface, with versitile tools for singel- and multivoxel MR spctrsocpy analysis, NMR signal processing, and simulation options. It is also capable of handling different sets of raw MRS data, such as Siemens, Phillips, Dicom data and many other common formats. The platform is widely used in both research and clinical settings for studying brain metabolism, cancer studies, and other applications in the field of magnetic resonance. [19]

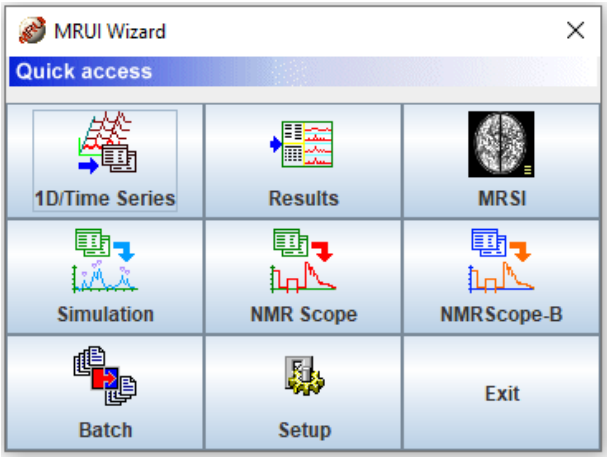

FIGURE 2.2: Overview of jMRUI platform displaying the 9 functions of the software.

Advanced Method for Accurate, Robust, and Efficient Spectral (AMARES) fitting is a quantitative toolbox offered in the jMRUI platform. AMARES can estimate metabolite concentrations from MR spectra acquired from various tissues and from different MRI vendors. The toolbox employs a non-linear fitting algorithm that models the acquired spectrum as a sum of individual metabolite resonances. The algorithm iteratively adjusts the metabolite model parameters to improve the fitting and find the least residuals of the experimental spectra and fitted ones.

The fitting process in AMARES considers several factors that can affect the accuracy and reliability of the results. It incorporates knowledge about the metabolite resonances' line shapes, frequencies, FWHM, and coupling patterns. Also, the algorithm includes methods to correct spectral artifacts, baseline distortion, and water, macromolecules, and lipid contaminations. There is also a section called

"prior knowledge" which allows the user to adjust frequencies, magnitude and line width from previously acquired knowledge for a better fit.

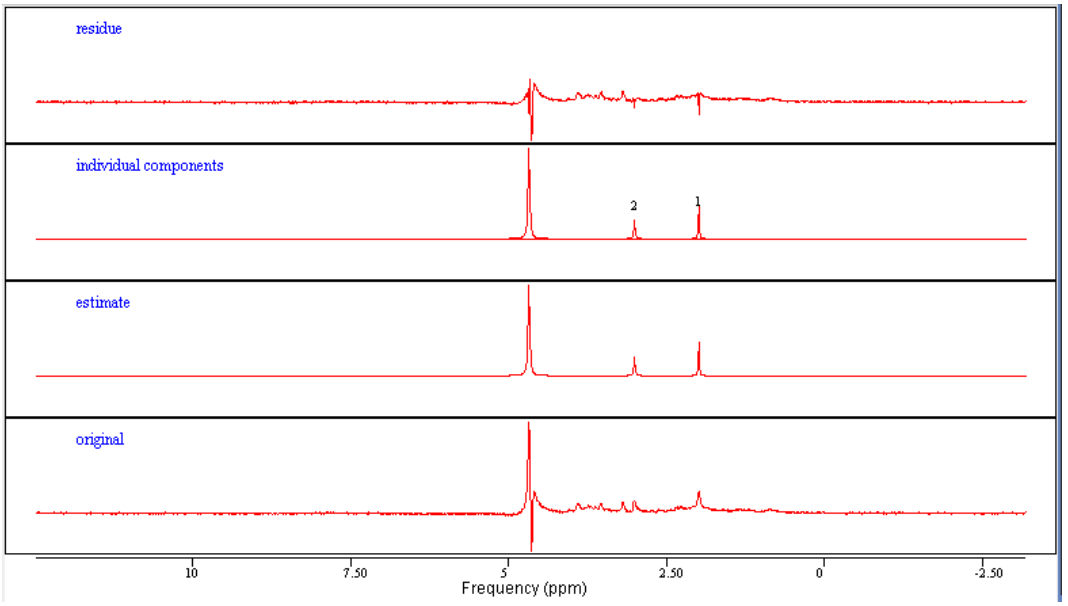

FIGURE 2.3: Example of fitting from raw MRS data processed by jMRUI where peak named 1 is NAA and the peak named 2 is Cr.

Figure 2.3 shows an example of jMRUI platform that enables the user to optimize different settings for better data visualization. It is possible to zoom, pick desired peaks and spectral fit data. This makes it a useful resource for uncovering patterns and extracting valuable information from data sets that might otherwise go unnoticed. In this particular example it is possible to see that metabolites are not properly fitted. This is especially the case when looking at NAA, there is negative spike in the residue that is clearly visible. For a better fit adjustments would have to be made in order to cancel out the negative signal in the residue. This could be achieved by further defining the frequency of NAA, and possibly making som sort of soft constraint. The same it true for Cr, the metabolites in between and the water signal itself.

As previously mentioned jMRUI harnesses the power of both *Lorentzian* and *Gaussian* distributions in quantifying data alongside a predefined model of spectra. This unique combination equips jMRUI with the ability to yield accurate results even from distorted or seemingly "random" data sets, setting it apart from other software options. However, this process demands a comprehensive understanding of data manipulation techniques to ensure that the results remain interpretable

without sacrificing data readability. Striking the right balance between manipulation and data integrity is crucial when working with jMRUI.

2.4 In vivo MRS

When dealing with tissue experiments prior knowledge of different metabolite concentrations is important. This is due to knowing a rough estimate of the ratio between metabolites when analyzing results, but also for detecting abnormalities in clinical use. Another important thing to point out is dealing with the water signal. Since around 60% of the human body is water the signal feedback from MRS is dominated by the water signal [3]. It is therefor important when in this case dealing with magnetic resonance spectroscopy imaging (MRSI) of the brain to cancel out the water signal.

2.4.1 Metabolites

Producing an MRS spectra can be done by using a multitude of metbolites such as ^{1}H, ^{31}P, ^{13}C and ^{23}Na each of which will generate a somewhat sensible spectra [11]. However, ^{1}H is considered being superior to work with because the hydrogen nucleus ^{1}H is highly sensitive to the magnetic resonance phenomenon, availability and concentration of it as a metabolite within the body. Moreover the equipment needed for this is readily available within most facilities that facilitates MR-scans.

Firstly it is important to define what a metabolite is in the context of the body. Metabolites are small molecules that play crucial roles in the metabolic processes of living organisms. They participate in various biochemical pathways and serve as important components for the formation of larger molecules, regulators of cellular activities, and molecules involved in intercellular communication. Metabolites encompass a diverse array of compounds, including sugars, amino acids, nucleotides, fatty acids, vitamins, hormones, and other organic substances.

Understanding the functions and roles of metabolites is vital for comprehending the intricate workings of cellular processes, discovering markers for diseases, and developing targeted therapeutic approaches. Analyzing metabolites provides a comprehensive perspective on the metabolic state of an organism, furnishing valuable information about its physiological and biochemical condition.

2.4.2 Metabolite biomarkers

The most common field strength in this application is considered to be between 1.5 and 3.0 tesla. 3.0 Tesla is generally seen as the better option when it comes to brain scans because of its higher image quality and shorter acquisition time. That being said, there are also some studies suggesting that 3.0 Tesla might give lesser results than 1.5 Tesla, this was espacially found to be the case when imaging the liver [16].

When it comes to the subject of selecting metabolites, it is estimated to be between 2,000 and 20,000 metabolites present in the body [2], of these there are especially 3 of interest, N-acetylaspartate(NAA), creatine (Cr) and choline(Cho). The reason for this is both the important processes of which each metabolite takes part in, but also the expected concentration of these at any given time. For example is NAA considered to be of high importance in the cells mitochondria. An unexpected increase or decrease could suggest something more sinister taking place where the abnormality is detected.

Tumor cells exhibit distinct metabolic profiles compared to their normal counterparts, reflecting adaptations that support their uncontrolled growth and survival. For example, the metabolic phenomenon known as the Warburg effect [13], where tumors exhibit altered glucose metabolism, is commonly observed. This effect involves increased glucose uptake and lactate production even in the presence of oxygen. Additionally, various other metabolites including amino acids, lipids, nucleotides, and intermediates of metabolic pathways are implicated in tumor metabolism [5].

By utilizing methods such as Magnetic Resonance Spectroscopy, researchers can explore these metabolic differences without invasive procedures. This allows for the analysis and characterization of specific metabolites in tumor tissues or biofluids, providing valuable insights into the rewired metabolism of cancer cells.

The spectral characteristics is also an important component when choosing a metabolite to quantify. Meaning that the metabolite in question should be easily distinguishable from other metabolites. When producing a spectra for lipids this is espacially the case, they are not as well defined as NAA is on a spectra and have a much wider signal (ppm). Figure 1 illustrates this by showing how some of the metabolits like NAA have much more prominent peaks than Glutamine (Gln).

2.5 MRS physics

Nuclear resonance is the process of measuring the energy absorbed in a given environment. To understand this we first have to look at what is meant by changes of energy on a atomic level. When looking at a isotope from a common element, a magnetic moment is present. Magnetic moment can be referred to as 'spin', meaning its rotational movement around its own axis. This property is what is effected and measured in a magnetic field. When the isotope nuclei is subjected to a constant magnetic field it might get excited, which is dependent to the orientation of the nucleus and the field. This causes the isotope to fluctuate between different energy levels. The rate of released energy from this fluctuation is the reaction that is being measured [6].

In equation (2.3) "v" represents the velocity or intensity of the frequency, "γ" represents the gyromagnetic ratio which is specific to a particular nucleus and "B_0" represents the applied magnetic field:

$$v = \frac{\gamma}{2\pi} \cdot B_0 \tag{2.3}$$

2.5.1 Magnetic fields

In MRS experiments, a robust and uniform magnetic field is applied to the sample under investigation. This field aligns the nuclear spins of specific atoms found in biological molecules, such as hydrogen (^{1}H) or carbon-13 (^{13}C). The alignment of these spins creates an overall magnetization parallel to the magnetic field direction. By introducing a second magnetic field, known as the radiofrequency field (RF), perpendicular to the primary magnetic field, the system can be perturbed. The RF field has the ability to excite the aligned nuclear spins, causing them to rotate around the magnetic field direction [10].

The rate of rotation, often referred to as the Larmor frequency, depends on the strength of the magnetic field and the inherent gyromagnetic properties of the observed nucleus. The gyromagnetic ratio, an intrinsic property of the nucleus, governs its sensitivity to the applied magnetic field.

The reliability and precision of MRS measurements rely on maintaining a stable and uniform magnetic field. Any fluctuations or non-uniformities in the magnetic field can introduce distortions in the spectra, consequently impacting the accurate quantification and interpretation of the signals related to metabolites.

2.5.2 Chemical shifts

When dealing with ^{1}H, the Chemical shifts can be explained as the magnetic field a proton is subjected to in its environment. The most relevant forces that applies to this is motion and density of surrounding electrons. Meaning that the composition of a molecule and how shielded the proton is by the surrounding electrons effects the chemical shift. For example, if the proton is shielded by a significant amount of electrons the frequency will be shifted 'up field', producing a frequency that is of a lower chemical shift. Whereas the opposite is true if the proton is shielded to a lesser degree.

When analysing MRS results one metabolite may have two different peaks. This appearance is due to an effect called Spin-Spin (T_2) Coupling. As previously mentioned each proton is affected by its local environment, this is not only relevant to electrons, but also other protons. The spin of a proton caused by its local environment can also effect another proton by making its magnetic moment to be slightly weaker or stronger. When examining this effect on a larger scale it becomes evident that roughly half of the neighboring protons are parallel and half perpendicular to the encompassing magnetic field. That is why the peaks on a spectrum can appear split, where the smaller peak appears to be shifted downstream somewhat. With this knowledge more precise measurements of each metabolite concentration can be made.

2.5.3 Spectrum and signal production

A core concept in signal formation is spin lattice (T_1) relaxation time and T_2 relaxtion time. T_1 can be described as the time it takes for the nuclear spins to return to their equilibrium relative to the environment. Meaning the time it takes for the longitudinal magnetization parallel to the affecting magnetic field to

recover from an external excitation. T_2 relaxtion time reffers to the time it takes for the transverse magnetization component to return to their equilibrium.

To achieve resonance for the purpose of detecting a characteristic signal, the weak oscillating field B_1 is superimposed onto the B_0 field. This works by creating a momentary high pulse similar to the frequency of the sample in question, which then will get amplified by oscillation and emitted by the sample temporarily until the system return to a equilibrium. From this process a signal is created called free induction decay (FID). After haveing obtained the FID signal a process known as *Fourier transformation* (FT).

$$F(\omega) = \int_{-\infty}^{\infty} f(t) \cdot e^{-i\omega t} dt \tag{2.4}$$

$$f(t) = \frac{1}{2\pi} \int_{-\infty}^{\infty} F(\omega) \cdot e^{i\omega t} d\omega \tag{2.5}$$

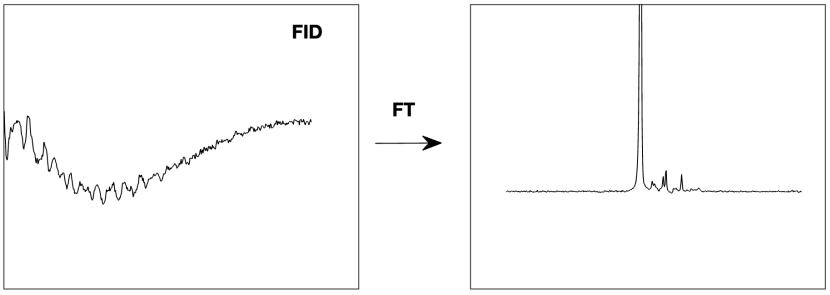

FIGURE 2.4: Illustration of how the obtained FID signal is decoded by using Fourier transformation (FT) to provide MR spectrum in frequency domain.

Chapter 3

Materials and Methods

3.1 MR Spectroscopy Data

We retrieved data from an openly available source provided by Archibald J. and colleagues [4]. This dataset includes MRS data for 15 participants undergoing a pain paradigm. The data were obtained using a 3 T Philips Achieva scanner (Best, Netherlands) with a single-channel Transmit-Receive head coil. Proton MRS data were acquired using PRESS localization sequence with the following parameters: echo time of 22 ms, repetition time of 4000 ms, 16 averages, a total scan time of 22 min and 4 sec, voxel size of $30 \times 25 \times 15$ mm^3, 2nd order shimming, and 16-step phase cycle with water suppression using the Excitation option.

3.2 Data Analysis Using jMRUI

JMRUI supports various file formats commonly used in MRS, allowing users to import and export data from different MRI systems. When working with the single-voxel MRS data, 1D/Time Series is chosen (**Figure 2.2**). The data was acquired on Phillips MR-scan resulting in the use of the Phillips format option in jMRUI.

Creatine peak was used as reference pivot to adjust the frequency range in ppm (**Figure 3.1**). Other metabolites were assigned with regards to the defined reference at 3.02 ppm. The line width (Hz) was automatically selected by the "Autopick" function in AMARES.

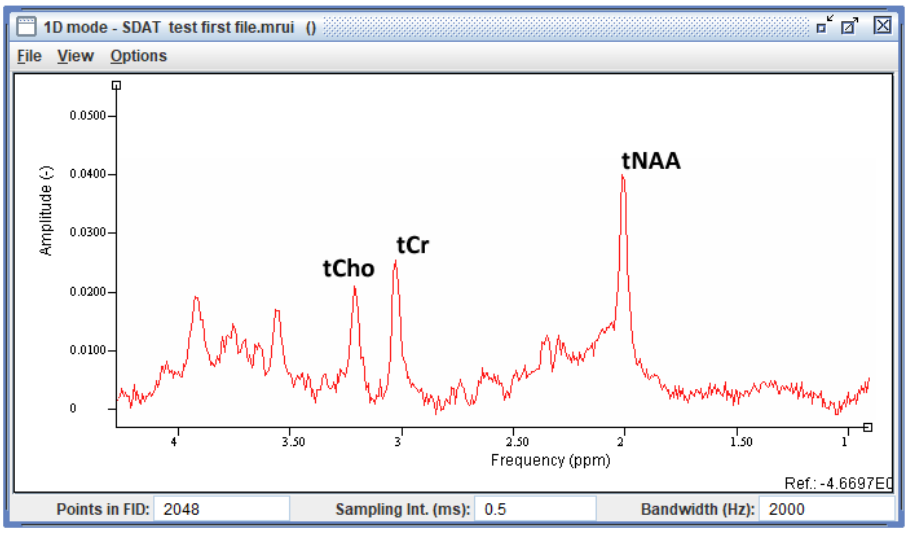

FIGURE 3.1: An example of MRS spectrum acquired from a healthy human brain. Abbreviation: tNAA, total N-acetyl aspartate; tCr, total creatine; tCho, total choline.

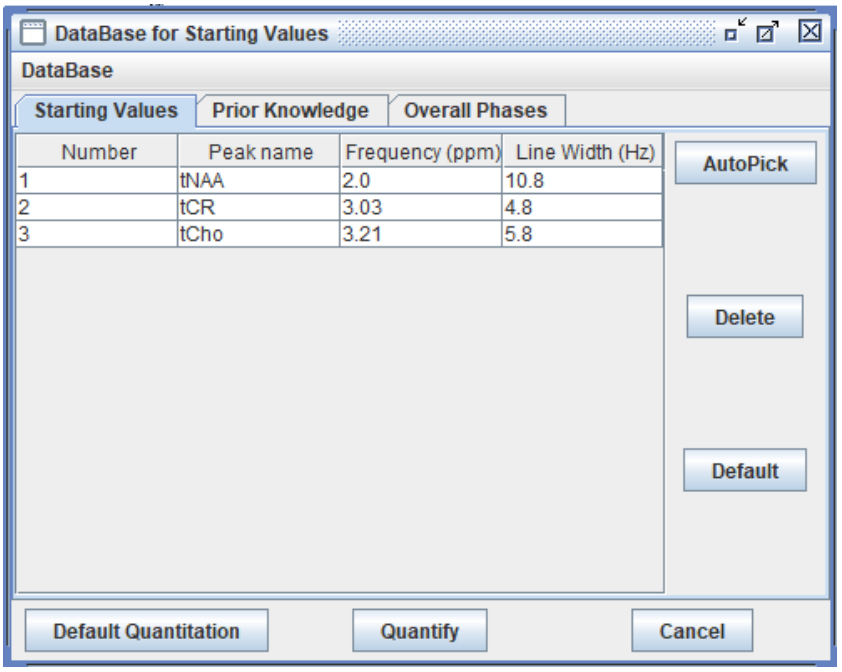

FIGURE 3.2: Starting values for NAA, Cr, and Cho in AMARES quantification.

Figures 3.2 and 3.3 illustrates the adjustments that were made to get a better fit. This was done for this particular data set, while other adjustments were made for separate data sets depending on their starting values. A trail and error approach was used when adjusting the fit for each individual MRS data set. *Lorentzian* and *Gaussian* distribution was used for all data sets.

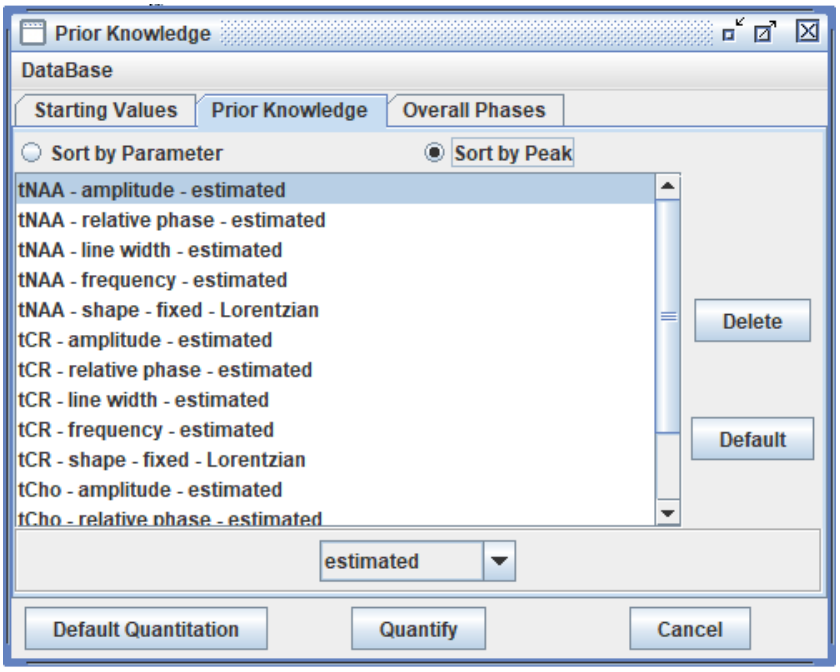

FIGURE 3.3: Prior knowledge section before any modifications.

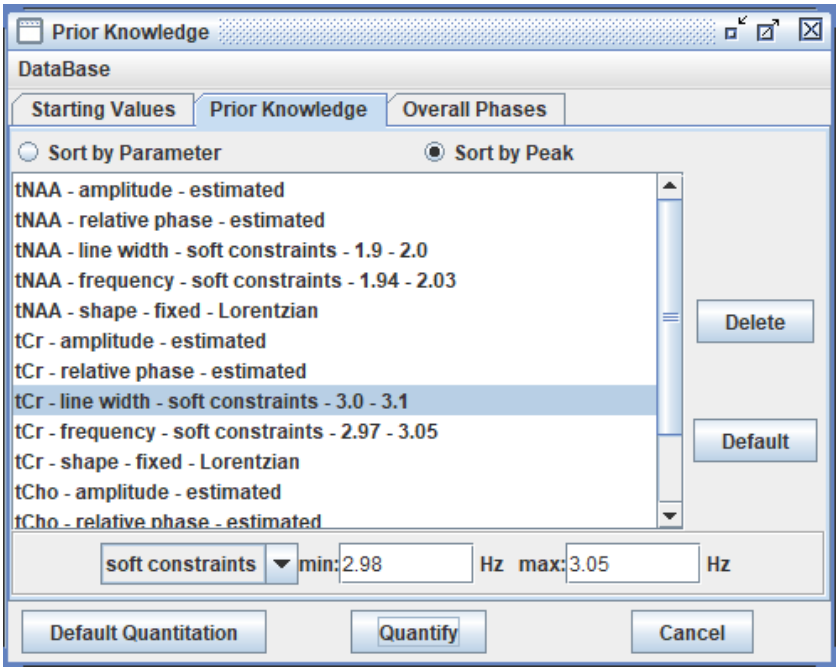

FIGURE 3.4: Prior knowledge section after modifications to NAA line width, NAA frequency, Cr line width, and Cr frequency.

(**Figure 3.4**) demonstrates how prior knowledge is an important factor in the success of quantification. Here, minor adjustments are made to the three metabolites in focus. This was done gradually until the damp was within a reasonable range and the residue had no significant peaks. This however is not always a straight forward process, and some adjustments may harm the end result. Therefor an understanding of the technical aspect to MRS as well as the biochemistry in the brain is crucial. Even though the results may look decent from a puerly technical point of wiev, the results may be unrealistic when looking at the ratio between certain metabolites. For example is NAA concentration expected to be higher than Cho concentration in a healthy brain. A deviation from this would be unexpected or potentially a sign of disease [15].

3.3 Preparation for LCModel analysis

In this study, LCModel was used to quantify MR spectra acquired from healthy brains. We set to investigate three important metabolites NAA, choline, and creatine. One essential requirement is preparation of suitable basis-set for the dataset. A conventional PRESS-sequence basis set with an echo time of 30 ms for a field strength of 3.0 T was selected. This basis-set provides an optimal prior knowledge for quantification of our data, simply because it would fit with the echo time and field strength of the acquisition setup. All spectra were analyzed from 0.8 to 4.2 ppm range to include metabolites of interest up to the water signal (**Figure 3.5**).

Because of the T_1 relaxation time and T_2 relaxtion time effect some metabolites can be located around more than one peak. It is also possible that a metabolite is bounded in more than one way, meaning that the signal may come from multiple peaks. For example was both Cr and Phosphocreatine (PCr) peaks counted when estimating the concentration. Another factor was the SD, which one of many factors that would indicate the accuracy of the result

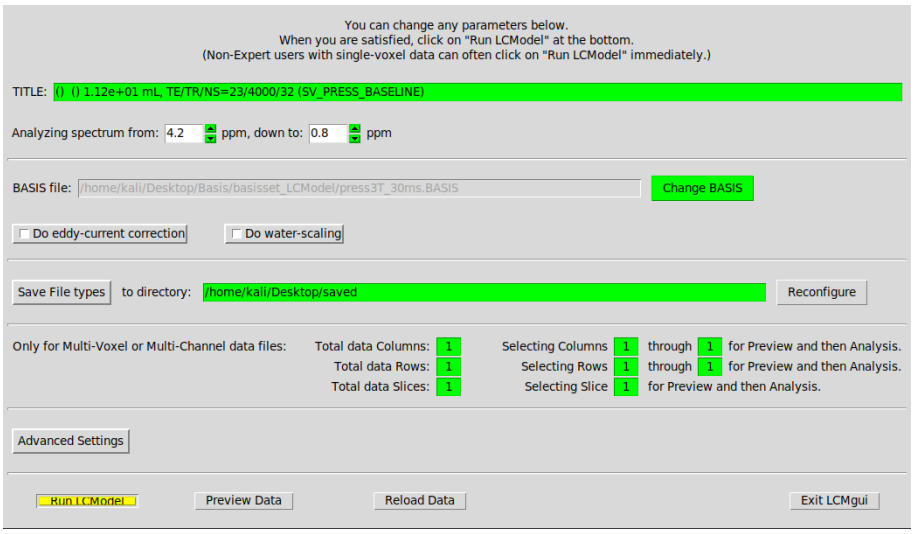

FIGURE 3.5: LCModels pre-render page displaying different settings and options for MRS quantification.

Conc.	%SD	/Cr+PCr	Metabolite
4.18E-05	107%	4.7E-02	Ala
8.07E-05	123%	9.0E-02	Asp
2.28E-04	41%	0.254	Cr
6.70E-04	**14%**	**0.746**	**PCr**
2.27E-04	31%	0.252	GABA
0.000	999%	0.000	Glc
2.76E-04	33%	0.307	Gln
4.80E-05	267%	5.3E-02	Glu
2.59E-04	**5%**	**0.288**	**GPC**
0.000	999%	0.000	PCh
1.60E-04	21%	0.178	GSH
3.77E-04	31%	0.419	Ins
1.45E-05	314%	1.6E-02	Lac
1.26E-03	**4%**	**1.406**	**NAA**
0.000	999%	0.000	NAAG
0.000	999%	0.000	Scyllo
4.03E-04	21%	0.449	Tau
0.000	999%	0.000	-CrCH2
2.59E-04	**5%**	**0.288**	**GPC+PCh**
1.26E-03	**4%**	**1.406**	**NAA+NAAG**
8.98E-04	**4%**	**1.000**	**Cr+PCr**
3.24E-04	44%	0.361	Glu+Gln

FIGURE 3.6: LCModels results, a multitude of metabolites, their concentration and SD.

Chapter 4

Results

4.1 Fitting Outcome Using jMRUI

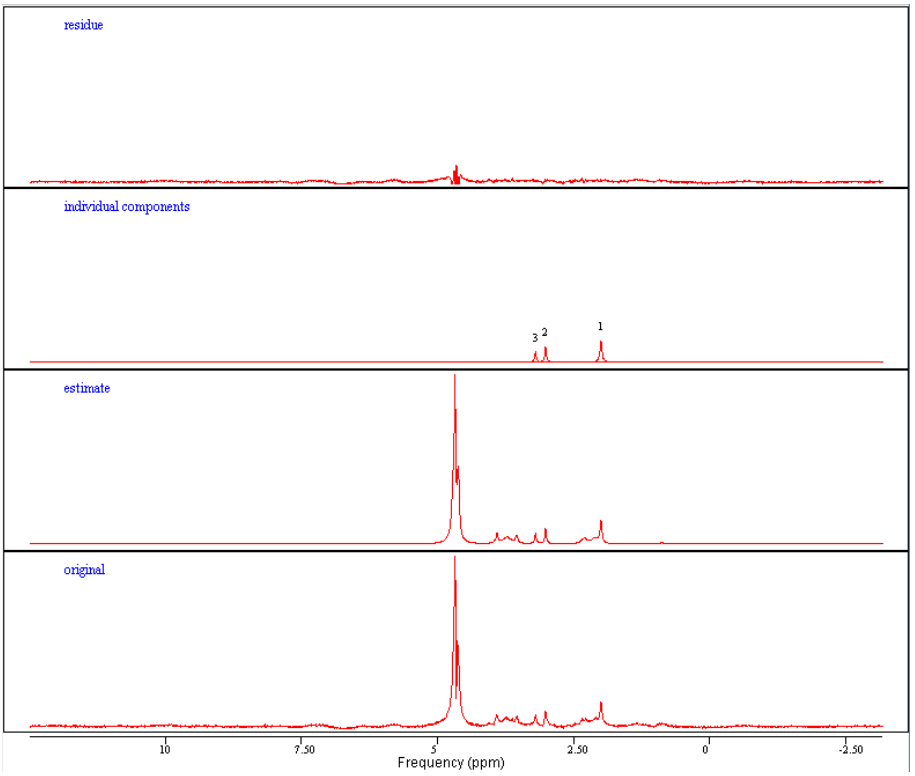

FIGURE 4.1: Result section in jMRUI with four spectra; residue, indivdual components, estimate and original. Peak 1 represents NAA, peak 2 is Cr and peak 3 Cho.

(**Figure 4.6**)

Name	Freq.(ppm)	Damp.(Hz)
1 - G tNAA	2.013	9.4
2 - G tCr	3.030	10.1
3 - G tCho	3.206	12.5

FIGURE 4.2: Quantification in jMRUI using Gaussian distrubution

Name	Freq.(ppm)	Damp.(Hz)
1 - L tNAA	2.013	15.6
2 - L tCr	3.030	16.8
3 - L tCho	3.206	20.8

FIGURE 4.3: Quantification in jMRUI using Lorentzian distrubution

(**Figure 4.2** and 4.3) Is an example showing how the use of two different distrubution methods impacted the result. In this case the use of *Gaussian* distribution benefited the accuracy of the result. This can be seen in the Damp(Hz) section where the spread is smaller when using *Gaussian*.

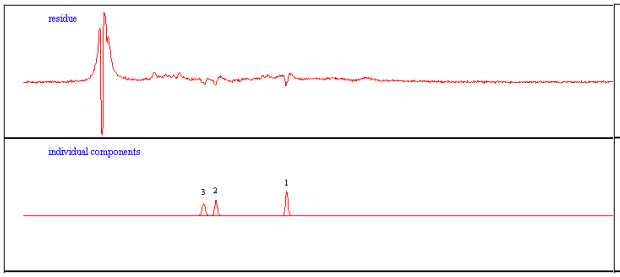

FIGURE 4.4: Quantification in jMRUI using Gaussian distrubution

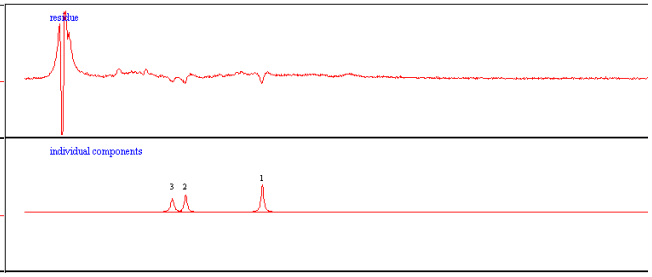

FIGURE 4.5: Quantification in jMRUI using Lorentzian distrubution

(**Figure 4.4** and 4.5) Illustrates the effect of distribution method visually. It becomes apparent that the width of the peaks are affected. In the example above it is what separates peak 2 and 3.

4.2 Fitting Outcome Using LCModel

From **Figure 3.6** Glycerylphosphocholine (GPC), NAA+N-Acetylaspartylglutamate (NAAG) and Cr+PCr was used to estimate concentrations. The blue color indicates a good fit based on SD. To set a reference point the difference between, the measured NAA concentration in subject 1 using jMRUI determined the ratio found in NAA concentration using LCModel. This ratio difference was then used on the other subjects and the metabolites in focus. By doing this it was possible to compare the results of jMRUI and LCModel.

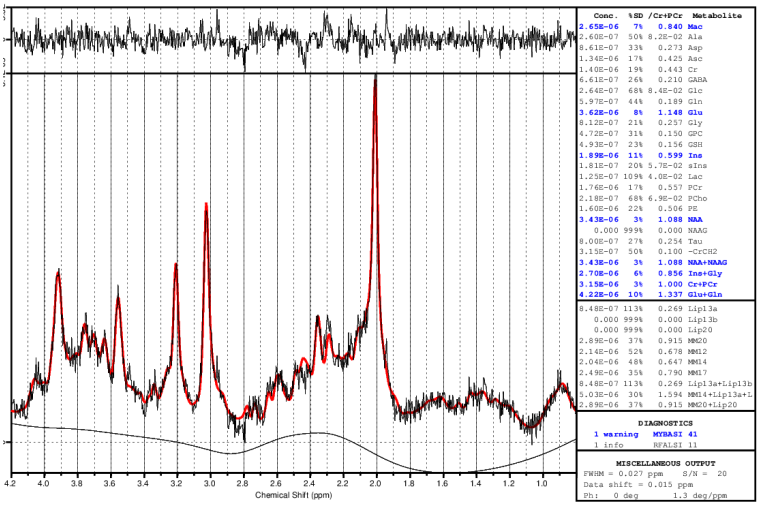

FIGURE 4.6: Result page in LCModel with multiple metabolites, SD and concentrations.

4.3 Fitting Outcome Comparison

Tests	jMRUI conc(E-04).			LCModel conc(E-04).			Total Deviation(%)
	NAA	Cr	Cho	NAA	Cr	Cho	%
1	7.55	2.49	2.12	7.55	2.28	2.59	3
2	4.35	2.37	1.84	4.35	1.98	1.42	17
3	3.73	1.97	1.37	3.73	2.00	1.13	7
4	3.31	2.61	7.19	3.31	2.00	7.28	10
5	4.77	2.29	1.66	4.77	2.48	1.33	6
6	2.67	2.33	2.38	4.08	2.34	2.74	16
7	2.75	1.89	1.65	2.75	2.68	7.41	31
8	2.85	1.54	1.27	2.65	2.20	7.41	16
9	2.11	3.02	2.92	2.53	2.39	5.48	247
10	3.59	2.74	2.12	2.83	2.77	7.06	75
11	3.86	2.59	2.31	3.37	1.97	8.04	78
12	2.62	2.42	1.68	2.96	3.08	4.46	81
13	3.08	3.02	2.75	1.57	4.16	3.23	59
14	2.87	2.06	1.65	2.99	2.04	7.27	41
15	2.91	1.33	2.58	2.42	2.22	3.33	318

The table above shows all the different concentrations estimated in jMRUI and LCModel for NAA, Cr and Cho for all the 15 subjects. The right most bracket compares the deviation between jMRUI concentration estimates and LCModel concentration estimates. This was done by first comparing each metabolite to

itslef across the two softwares. After this was done for all three the joint deviation was summed up and divided by 3 to get the final total deviation. The colors indicate the goodness of the fit, were values with no colors are decent, yellow colored values are bad and red colored values are unusable because of the large discrepancy between the concentrations. The color scale that is purposed was inspired by the research article "Comparison of seven modelling algorithms for γ-aminobutyric acid–edited proton magnetic resonance spectroscopy", but with the scale range being even larger due to Cho fitting. [1]

4.4 Conclusion

The results from the fitting outcome comparison shows similar deviations with a few exceptions. When looking at the average deviation the result shows 67%, but by removing the deviation numbers marked in red we get 34% deviation, and by removing the deviation marked in yellow we get 21% deviation.

When analyzing each individual metabolite the results indicate that NAA was overall the best fitted metabolite closely followed by Cr. By looking at the goodness of the fit between the first two (NAA and Cr) metabolites and the third metabolite (Cho) it is obvious that Cho is fitted the worst, by far.

Chapter 5

Discussion and Conclusion

As mentioned in the result section of this thesis it is obvious that Cho is poorly fitted. It is so poorly fitted when comparing it to the two different software that the data would be unusable any kind of data of fitting analyzing. Factors that might have caused this seems to be connected to LCModel. This suspicion is based on some of the metabolite ratios found in LCModel, whereas the source of an error was easier to identify when working with jMRUI because the visual representation of residue and personally picking peaks from a known refrence point. A viable solution to this problem might be to change the basis set. Although I found many basis sets, I could not find a basis set that matched the ET perfectly. This may have caused the misleading concentration results of the metabolites, which affected Cho in particular.

To identify the source of the problem different quantification methods could also have been used, as it is hard evaluating the origin of the mistake when only having two sources. Multiple quantification methods would possibly have made it easier to uncover if the mistake was due to choosing the wrong basis set or if the error was caused by the user.

On the subject of having to choose between multiple basis sets, problems of implementing MRS in a clinical setting may arise. When dealing with different ET and field strengths it might be difficult to choose the right basis set without having a good understanding of the technical aspects of MRS. On the other side lacking knowledge about biochemistry and metabolomics might also lead to complications when dealing with MRS data.

Therefor I wish to highlight this possible problem so that the potential of MRS can be utilized. There are few techniques that can collect valuable data from

tissues like the brain whilst being non-invasive. Its potential in both uncovering small changes in metabolic activity, but also the metabolic activity in reaction to a stimuli makes it applicable for learning purposes about the brain as a whole. Due to some of the obstacles I have discussed in this thesis the method of MRS has gone unnoticed by the clinical community and as a result been underused, not reaching its possible potential. In the future, it is therefor important to further implement more standardized techniques.

List of Figures

Bibliography

[1] Craven A.R., Bhattacharyya P.K., and Clarke. W.T. "Comparison of seven modelling algorithms for γ-aminobutyric acid–edited proton magnetic resonance spectroscopy". In: *John Wiley Sons Ltd* DE210100790 (2022). DOI: 10.1002/nbm.4702.

[2] Schmidt C.W. "Metabolomics: what's happening downstream of DNA." In: *Environ Health Perspect* (2004). DOI: 10.1289/ehp.112-a410.

[3] Mitchell H.H. et al. "THE CHEMICAL COMPOSITION OF THE ADULT HUMAN BODY AND ITS BEARING ON THE BIOCHEMISTRY OF GROWTH*". In: *Division of Animal Nutrition, and the Departments of Phpiology and Animal Husbandry* (1945), pp. 625–637.

[4] Archibald J. et al. "Metabolite activity in the anterior cingulate cortex during a painful stimulus using functional MRS". In: *Scientific Reports* (2022). DOI: 10.1038/s41598-020-76263-3.

[5] García-Cañaveras J.C. and Tumor L.A. "Tumor Microenvironment-Derived Metabolites: A Guide to Find New Metabolic Therapeutic Targets and Biomarkers". In: *Trend in Biochemical Sciences* 28 (2021). DOI: 10.3390/cancers13133230.

[6] Tognarelli J.M. et al. "Magnetic Resonance Spectroscopy: Principles and Techniques: Lessons for Clinicians". In: *Clinical and Experimental Hepatology* (2015). DOI: 10.1016/j.jceh.2015.10.006.

[7] Alger J.R. "Encyclopedia of Neuroscience". In: *Academic Press* (2009), pp. 601–607. DOI: 10.1016/B978-008045046-9.00300-4.

[8] Alger J.R. "Neurobiology of Disease". In: *Academic Press* (2007), pp. 781–792. DOI: 10.1016/B978-012088592-3/50074-8.

[9] Emsley J.W. and Feeney. J. "Forty years of Progress in Nuclear Magnetic Resonance Spectroscopy". In: *Elsevier* DE210100790 (2007), pp. 179–198. DOI: 10.1016/j.pnmrs.2007.01.002.

[10] Cuypers K. and Marsman A. "Transcranial magnetic stimulation and magnetic resonance spectroscopy: Opportunities for a bimodal approach in human neuroscience". In: *NeuroImage* 224 (2021). DOI: 10.1016/j.neuroimage.2020.117394.

[11] van der Graaf M. "In vivo magnetic resonance spectroscopy: basic methodology and clinical applications". In: *Springer* (2009), pp. 527–540. DOI: 10.1007/s00249-009-0517-y.

[12] Osorio-Garcia M.I. et al. "Quantification of in vivo 1 H magnetic resonance spectroscopy signals with baseline and lineshape estimation Quantification of in vivo 1 H magnetic resonance spectroscopy signals with baseline and lineshape estimation". In: *Measuremnet Science and Technology* 22 (2011). DOI: 10.1088/0957-0233/22/11/114011.

[13] Liberti M.V. and Locasale J.W. "The Warburg Effect: How Does it Benefit Cancer Cells?" In: *Trend in Biochemical Sciences* 41 (2016), pp. 211–218. DOI: 10.1016/j.tibs.2015.12.001.

[14] Mansfield P. and Maudsley A.A. "Medical Imaging by NMR". In: *Br J Radiol* 50.591 (1977 Mar), pp. 188–194. DOI: 10.1259/0007-1285-50-591-188.

[15] Pouwels P.J. and Frahm J. "Regional metabolite concentrations in human brain as determined by quantitative localized proton MRS". In: *Magn Reson Med* 39 (1998), pp. 53–60. DOI: 10.1002/mrm.1910390110.PMID:9438437.

[16] Girometti R. "3.0 Tesla magnetic resonance imaging: A new standard in liver imaging?" In: *World J Hepatol* (2015). DOI: 10.4254/wjh.v7.i15.1894.

[17] Kreis R. "Issues of spectral quality in clinical 1H-magnetic resonance spectroscopy and a gallery of artifacts". In: *NMR Biomed* 17 (2004), pp. 361–381. DOI: 10.1002/nbm.891.

[18] Provencher S. *LCModel1 LCMgui User's Manual*. Version 6.3-1R. s-provencher, 2021.

[19] *SpectraClassifier 3.1.1 jMRUI plugin Help and Manual*. Universitat Autònoma de Barcelona, 2013.

[20] Jain V., Biesinger M.C., and Linford M.R. "The Gaussian-Lorentzian Sum, Product, and Convolution (Voigt) functions in the context of peak fitting X-ray photoelectron spectroscopy (XPS) narrow scans". In: *Elsevier* 447 (2018), pp. 548–553.